The Journal of Experimental Biology 212, 3511-3521
Published by The Company of Biologists 2009
doi:10.1242/jeb.033886

Whole limb kinematics are preferentially conserved over individual joint kinematics after peripheral nerve injury

Young-Hui Chang[1,*,†], Arick G. Auyang[2], John P. Scholz[3] and T. Richard Nichols[1,*]

[1]Department of Physiology, Emory University School of Medicine, Atlanta, GA 30322 USA, [2]School of Applied Physiology, Georgia Institute of Technology, Atlanta, GA 30332-0356, USA and [3]Department of Physical Therapy, University of Delaware, Newark, DE 19716, USA

*Present address: School of Applied Physiology, Georgia Institute of Technology, Atlanta, GA 30332-0356, USA
[†]Author for correspondence (yh.chang@ap.gatech.edu)

Accepted 30 July 2009

SUMMARY

Biomechanics and neurophysiology studies suggest whole limb function to be an important locomotor control parameter. Inverted pendulum and mass-spring models greatly reduce the complexity of the legs and predict the dynamics of locomotion, but do not address how numerous limb elements are coordinated to achieve such simple behavior. As a first step, we hypothesized whole limb kinematics were of primary importance and would be preferentially conserved over individual joint kinematics after neuromuscular injury. We used a well-established peripheral nerve injury model of cat ankle extensor muscles to generate two experimental injury groups with a predictable time course of temporary paralysis followed by complete muscle self-reinnervation. Mean trajectories of individual joint kinematics were altered as a result of deficits after injury. By contrast, mean trajectories of limb orientation and limb length remained largely invariant across all animals, even with paralyzed ankle extensor muscles, suggesting changes in mean joint angles were coordinated as part of a long-term compensation strategy to minimize change in whole limb kinematics. Furthermore, at each measurement stage (pre-injury, paralytic and self-reinnervated) step-by-step variance of individual joint kinematics was always significantly greater than that of limb orientation. Our results suggest joint angle combinations are coordinated and selected to stabilize whole limb kinematics against short-term natural step-by-step deviations as well as long-term, pathological deviations created by injury. This may represent a fundamental compensation principle allowing animals to adapt to changing conditions with minimal effect on overall locomotor function.

Key words: walking, locomotion, biomechanics, nerve injury, reinnervation.

INTRODUCTION

In nature, animals maintain stable legged locomotion despite encountering unpredictable terrain from one step to the next. Adjustments are regularly made to counteract naturally occurring joint deviations and may go unnoticed with casual observation. When a limb is injured, however, individual joint function can be compromised and this can lead to noticeable deficits. The ability to exploit a pre-existing compensation mechanism for counteracting joint deviations and conserving normal whole limb function may help retain locomotor performance after injury. Intralimb gait compensation involves responses of some joints that act to attenuate the effects of deficits at other joints. This assumes that a task level goal, such as consistency of whole limb kinematics, guides the overall compensation process.

Findings from biomechanical and neurophysiological studies suggest that conserving limb-level function is an important goal during locomotion. For decades, researchers have studied steady state legged locomotion to yield biomechanical models that predict the locomotor dynamics of walking and running gaits across diverse taxonomic groups. The inverted pendulum model for walking (Cavagna et al., 1977; Griffin et al., 2004) and the mass-spring model for running (Blickhan, 1989; McMahon and Cheng, 1990) each provide low-degree of freedom behavioral templates that can describe whole body movements during legged locomotion (Full and Koditschek, 1999). These biomechanical models reduce the neuromusculoskeletal complexity of the legs to the simple function of a rigid strut or a linearly elastic spring rotating about a point mass. Neurophysiological studies also support a neural basis for the importance of limb-level function in locomotion. Recent studies have indicated that the central nervous system directly encodes whole limb kinematics rather than individual joint kinematics. Dorsal spinocerebellar tract (DSCT) neurons in the cat spinal cord integrate and carry sensory information to the cerebellum and are known to influence locomotion and posture. *In vivo* recordings from these DSCT neurons revealed that the majority of the ascending DSCT activity reflected the cat's overall limb orientation and limb length kinematics rather than providing specific information about an individual joint (Bosco and Poppele, 2000; Bosco and Poppele, 2003; Bosco et al., 2000). Although the importance of whole limb behavior to locomotion is clear, we do not have a good understanding about how the joints act in concert to conserve limb-level function during locomotion and particularly whether such a compensation strategy is engaged after neuromuscular injury.

In the cat, surgical transection and immediate repair of individual nerves supplying the muscles of the triceps surae group of ankle extensors reliably results in a brief paralytic stage of approximately one month followed by complete self-reinnervation of the affected muscles after 9–12 months (Cope et al., 1994; Cope and Clark, 1993). The self-reinnervated muscle regains full efferent motor function with a permanent disruption of the short-latency, proprioceptive reflex pathways from the reinnervated muscle commonly referred to as the monosynaptic stretch reflex. This peripheral nerve injury results in increased ankle joint flexion, or yield, during the initial weight-bearing portion of the

stance phase of gait when the muscle is in the paralytic stage (Abelew et al., 2000; Maas et al., 2007). After self-reinnervation, measurable joint-level deficits can persist for years after the injury, particularly during down-slope walking when engaging the short-latency pathways are more critical to joint function. These studies have focused on the deficits to joint range of motion rather than comparing joint function relative to whole limb function over the entire gait cycle. We used this surgically precise, peripheral nerve self-reinnervation model to gain insights into locomotor compensation strategies at different stages of injury and recovery. This approach also allowed us to compare injuries across different muscles as a first test of the fundamental nature of these compensation principles.

Our main objective was to test the general hypothesis that a locomotor compensation strategy exists such that joint angle combinations are selected that achieve consistency, or a minimum change, in limb kinematics (see Fig. 1). We made two predictions related to our general hypothesis about both long-term locomotor compensation and short-term locomotor compensation. First, we defined long-term compensation as the conservation of mean limb kinematics trajectories across all individuals at the expense of changes to mean joint kinematics trajectories. We tested this long-term compensation by comparing the consistency of the mean trajectory shapes of limb and individual joint kinematics after neuromuscular injury. We predicted that the majority of the mean post-injury limb kinematics trajectory could be explained by the pre-injury kinematics for all cats (R^2>0.50), whereas the mean joint angle trajectories would follow new and different trajectories resulting in lower R^2 values. Second, we defined short-term compensation as the minimization of the step-by-step variance of limb kinematics that is concomitant with an increased variance in joint kinematics. We tested for short-term compensation by comparing the total variance of limb orientation and joint angles on a step-by-step basis. We predicted that total variance of the joint angles would be greater than that for limb orientation, indicating that the combined effect of these greater step-by-step joint angle deviations is to counteract and minimize deviations in limb orientation.

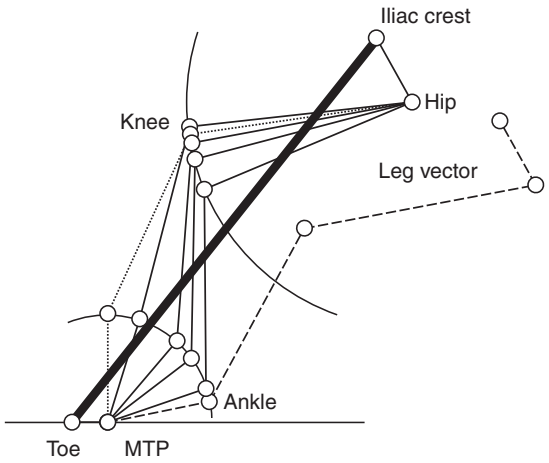

Fig. 1. Diagram of hindlimb segments oriented with several hypothetical joint angle combinations (thin solid lines) that satisfy the same general limb position goal (thick solid line). There are many joint angle combinations that do not achieve the goal position (dashed lines) and still other combinations that are prevented because of musculoskeletal limitations (dotted lines).

MATERIALS AND METHODS

Animal care and training

We performed all procedures according to an approved protocol by the Emory University Institute for Animal Care and Use Committee. Five adult cats (*Felis catus* L.; mean body mass=3.91±0.64 kg) were selected based on friendliness and ability to train for food rewards. All animals were socially housed in a colony within a single large room that exceeded NIH recommendations for space requirements (Institute for Laboratory Animal Research, 1996). Dry food and water were provided *ad libitum* within the colony; treadmill locomotion training rewards consisted of wet food.

We trained the animals over a 1–3 month period until they could walk on command at 0.8 m s^{-1} for a minimum of 60 s on a custom treadmill. Food rewards were given after each completed trial. We constructed the treadmill frame from an extruded aluminum chassis (Varco, Greenwood, SC, USA) with a 0.32 cm thick aluminum bed supporting a low-friction 0.32 cm Teflon surface (Fluoro-Plastics, Philadelphia, PA, USA) over which a 0.24 m wide treadmill belt (Regional Supply, Marietta, GA, USA) could easily slide. A 0.5 hp DC brushless motor with reversible digital controller and speed readout (Cole Electric, Atlanta, GA, USA) turned a custom-lathed aluminum drive shaft. The general treadmill construction followed a design similar to one previously developed for human studies (Kram et al., 1998), but was appropriately scaled to the dimensions of a cat. A clear acrylic enclosure (0.95 m×0.34 m×0.62 m) was constructed to fit over the treadmill without affecting belt movement. An additional adjustable wall-spacer further restricted lateral position on the treadmill such that the walking surface for each cat was approximately 0.16 m×0.95 m to ensure steady, forward locomotion.

Self-reinnervation procedure

A peripheral nerve injury was generated in each animal through a previously described surgical procedure (Cope et al., 1991). Briefly, the cat was placed under general anesthesia (isoflurane gas) within a sterile surgical field. We exposed the tibial nerve with a longitudinal incision in the popliteal fossa of the left hindlimb. We then identified the distal-most portion of the nerve branch innervating the lateral head of the gastrocnemius and soleus muscles. Through a dissecting microscope, we cut the epineurium and divided the approximately three to four individual nerve bundles supplying the soleus muscle for two cats. We verified the innervation of these nerve bundles through electrical stimulation of the bundles with bipolar hook electrodes. For the three remaining cats, in addition to the soleus the individual nerve branches innervating the lateral and medial heads of the gastrocnemius muscle were also identified in a similar fashion. Each of the individual nerve branches (or bundles) identified during surgery was independently transected and the cut ends were immediately reattached with 10-0 non-absorbable monofilament suture (S&T AG, Neuhausen, Switzerland). Since these nerve branches and bundles were cut and reattached at their most distal point of entry into the muscle belly, we minimized any chance of cross-reinnervation into an inappropriate muscle as is common for injuries made proximal to major branch points (English, 2005). While in the operating room, we verified the loss of innervation to the muscle through electrical stimulation of the individual nerve branches proximal to the repair site. We did not observe any response from repaired muscles but did observe clear activation when testing neighboring unaffected muscles. Consequently, the wound site was closed using sterile sutures and the cat was allowed to heal in isolation over the next 7 days, after which the animal was returned to the general colony. Although it was not critical

to the hypotheses directly tested in this study, we later verified the sensory loss in the reinnervated muscle during a terminal procedure using a well-described method (Huyghues-Despointes et al., 2003a; Huyghues-Despointes et al., 2003b; Nichols, 1989; Nichols, 1999). Also during the terminal procedure, we directly measured hindlimb bony segment lengths for use in our kinematics model and independently weighed the four major ankle extensor muscles (soleus, medial and lateral gastrocnemius heads, and plantaris muscles) from both hindlimbs to test for symmetry.

Hindlimb kinematics

Prior to any behavioral testing, the cats were injected intramuscularly with 0.06 mg kg^{-1} of medetomidine (Domitor®, New York, NY, USA), a reversible veterinary sedative-analgesic commonly used for minor diagnostic procedures not requiring general anesthesia. While sedated, the animals' hindquarters were shaved to allow for accurate palpation and ink marking of anatomical landmarks. Regardless of animal size, we intramuscularly injected 0.10 ml of atipamozole (Antisedan®, Pfizer) to reverse the effects of the medetomidine. Cats were typically alert, upright and walking within 10–20 min of injection of the reversal agent. With the cat in a standing position and using the marked skin as a guide, we attached retroreflective markers to the skin at the superior iliac crest, greater trochanteric notch, lateral epicondyle of the femur, lateral malleolus of the fibula, fifth metatarsal head, and the proximal interphalangeal joint of the left leg (Fig. 2).

Pre-injury control data were collected on two separate days before the nerve injury surgery was performed. Post-injury data were collected 1-month post-surgery during the muscle paralytic stage and at 14 months post-surgery during the muscle self-reinnervated stage. The self-reinnervated stage data reported here reflect the 14-month post-injury stage for all but one cat, which did not complete the 14-month collection. Instead, 9-month self-reinnervated stage data were successfully collected and are reported for this individual. During all data collection trials, the cats walked on our treadmill at 0.8 m s^{-1} until a steady gait was observed. Three-dimensional (3-D) marker positions on the left hindlimb were recorded at 125 Hz for 16 s with a two-camera motion capture system (Peak Performance Technologies, Denver, CO, USA) and saved to a computer for later analysis. Animals were allowed to rest for at least 2–5 min between the two to four trials collected for each day of collection. A typical 16-s trial consisted of approximately 25 stride cycles; however, we excluded any portions of a trial that was not at constant speed to minimize any acceleration effects. Although constant speed was a criterion for data inclusion, this did not require the animals to place their paws on the treadmill belt in the same relative anteroposterior position with each step. Given the general relationship between speed, step frequency and step length, an infinite number of different limb orientations at ground contact could have resulted in the same constant walking speed. Additionally, for any given limb orientation, an infinite number of limb lengths can be achieved by simply varying the joint angles in an accordion-like fashion. It is important to point out that the mechanics of constant speed treadmill locomotion are identical to that of over ground locomotion (van Ingen Schenau, 1980) and results in comparable kinematics and kinetics (Riley et al., 2007). Therefore, it is reasonable to expect numerous options with respect to limb positions and kinematics trajectories over the step cycle as one might during over ground locomotion. The data from all trials were pooled for each condition and on average we analyzed 38 steps (±25; ±s.d.) per cat and condition with a range of 17–100 strides across all cats and conditions.

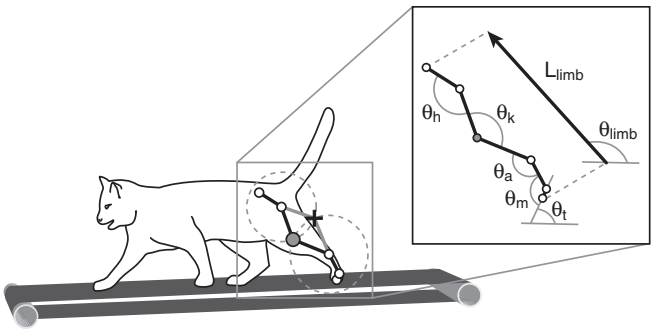

Fig. 2. Schematic of cat walking on treadmill. Reflective skin markers (open circles) placed over the (proximal to distal): iliac crest, greater trochanter, lateral malleolus, fifth metatarsal head and the fifth distal phalanx. During postmortem dissection, we directly measured femoral and tibial segment lengths (represented by the radius of each gray dashed circle). These segment lengths were used along with the hip and ankle joint positions to solve for the two intersection points of the femur and tibia (filled circle and cross) at each time point of the gait cycle. Only one solution represented an anatomically viable solution (filled circle). Inset: angle definitions for hip (θ_h), knee (θ_k), ankle (θ_a) and MTP (θ_m) joints along with toe segment angle (θ_t) and the limb orientation (θ_{limb}) and limb length (L_{limb}) of the toe-to-hip vector.

Marker position data were low-pass filtered (zero-lag, fourth order Butterworth filter, 7 Hz cut-off) and reconstructed to 3-D positions using commercial motion analysis software (Peak Motus 8.0, Peak Performance Technologies, Denver, CO, USA). The sagittal plane knee joint center was determined by calculating the two intersection points of two circles whose centers were defined by the hip and ankle joints and whose radii were defined by the segment lengths of the femur and tibia, respectively (Fowler et al., 1993; Goslow et al., 1973). From these two points of intersection, only one provided an anatomically appropriate solution and was used as the knee joint center. From the marker positions, 2-D sagittal plane joint angles were calculated for the hip, knee, ankle and metatarsalphalangeal (MTP) joints (Fig. 2). We performed a subsequent check on our data to verify that out-of-plane limb movements were minimal. The animals were killed with an overdose of sodium pentobarbital (Nembutal, 150 mg kg^{-1}), and the hindlimb was dissected and bone segment lengths of the femur and tibia were directly measured to use in our knee triangulation procedure. Using calipers, we measured the femoral segment length as the distance between the center of the femoral head to the estimated knee joint center between the lateral femoral epicondyle and lateral tibial plateau. We measured the tibial segment length as the distance between the same point between lateral femoral epicondyle and lateral tibial plateau to the apex of the lateral malleolus of the fibula. We defined the whole limb position as a vector drawn from the toe marker to the pelvic marker (Fig. 2). From this limb vector, we could calculate the kinematics of the limb orientation and limb length over each gait cycle. The trajectories of each joint angle and limb position component were then time-normalized and averaged over the gait cycle.

Anatomical measurements

All cats showed morphological symmetry across right and left hindlimbs with respect to bony segment lengths and post-injury muscle masses. Our cadaveric measurements after the terminal procedure yielded nearly symmetrical hindlimb segment lengths for all animals with the greatest mean difference between left and right

Table 1. Anatomical measurements

	Cat 1	Cat 2	Cat 3	Cat 4	Cat 5	Mean difference from right (s.d.)
Body mass (kg)	3.15	3.60	3.95	4.90	3.94	
Left limb segment (cm)						
Pelvis	5.77	6.03	6.11	5.55	5.67	0.05 (0.14)
Femur	9.73	9.50	11.00	10.57	10.00	–0.16 (0.29)
Tibia	11.30	11.00	12.20	12.20	10.55	0.09 (0.06)*
Tarsus	6.55	6.80	7.10	6.87	6.77	–0.08 (0.16)
Hallux	1.55	1.60	1.80	1.90	1.39	0.04 (0.04)
Right limb segment (cm)						
Pelvis	5.70	5.90	6.03	5.40	5.87	
Femur	9.60	9.70	10.90	10.83	10.57	
Tibia	11.20	11.00	12.07	12.15	10.39	
Tarsus	6.70	6.70	7.10	6.90	7.09	
Hallux	1.53	1.50	1.73	1.90	1.35	
Left muscle mass (g)						
Medial gastrocnemius	9.57	10.66	12.51	17.53	9.44	–0.38 (1.04)
Lateral gastrocnemius	11.81	11.90	11.13	17.54	11.36	–1.42 (1.42)
Soleus	3.94	3.78	6.51	5.15	3.98	0.14 (0.64)
Plantaris	6.80	6.08	7.81	10.10	8.45	0.09 (0.63)
Right muscle mass (g)						
Medial gastrocnemius	9.57	10.95	13.73	16.43	10.95	
Lateral gastrocnemius	12.17	12.02	14.32	18.27	14.08	
Soleus	4.06	3.77	5.43	5.78	3.60	
Plantaris	6.74	6.49	8.32	9.83	7.40	

*Significant asymmetry, $P<0.05$.

segment lengths measuring only 1.6±2.9 mm (Table 1), which we did not find to be significant ($P=0.28$). We found a small but significant difference of 0.9±0.6 mm in the left tibial segment ($P=0.04$) Nevertheless, this difference amounted to less than a 1% difference in segment length. The mean differences for all respective segments of the left and right limbs averaged less than 3%. The ankle extensor muscle masses from the affected left hindlimb did not show any asymmetries across cats when compared with their corresponding muscle in the contralateral limb (Table 1). We observed the largest difference in the lateral gastrocnemius muscle mass, with that of the left limb being on averaged 1.4 g lighter than that of the right limb, resulting in a 12% difference that was not statistically significant ($P=0.09$). We verified, through video observation, that all cats walked with symmetrical gait patterns for all trials and conditions. The overall symmetry in muscle masses also suggests that there were no gross architectural changes related to asymmetric gait patterns, such as atrophy or hypertrophy in the affected muscles or their synergists.

Long-term compensation: consistency of mean kinematics trajectories after injury

We calculated the means of the kinematics trajectories across all strides for each cat and condition (Matlab, Natick, MA, USA). We quantified the consistency of the mean post-injury kinematics data relative to the mean pre-injury kinematics by performing linear regressions on each of the two sets of mean post-injury trajectories (Paralytic and Self-Reinnervated Stages) versus the mean pre-injury trajectories (Matlab). We performed these linear regressions over the initial yield phase of stance as determined by the ankle joint (~15% of stride) and also over the entire stance phase (~60% of stride). We then used the coefficient of determination (R^2) from each variable regression to quantify the consistency of the mean kinematics trajectory after injury for one animal. The R^2 values were then averaged across all cats at each injury stage ($\bar{R}^2$). If $\bar{R}^2>0.50$, then we could say that the majority of the trajectory shape after injury can be explained by the same pattern observed before injury for all cats (one-tailed, *t*-test, $\alpha=0.05$, JMP, SAS Institute, Cary, NC, USA). This metric allowed us to test whether the trajectory of each of the kinematics variable persisted after injury and whether this was a common feature across all cats. Mean kinematics trajectories over multiple steps provide us with an estimate of what the kinematics goals may be during locomotion. Comparing pre-injury mean trajectories to their corresponding post-injury data would indicate whether the kinematic targets for that variable had changed due to the injury.

Short-term compensation: step-by-step variance of kinematics variables

We calculated the variance of the different kinematics variables defined in our hindlimb model (Fig. 2) across all strides for each cat and condition. We then cumulatively summed the variance over the entire stride cycle to obtain a single metric we termed ‘total variance’. We compared total variance for each joint angle and for limb orientation angle across all cats and data collection stages (pre-injury, paralytic stage, and self-reinnervated stage). Pooling variance data across all joints and recalculating a single mean total variance value for all joints, we performed a one-tailed *t*-test to assess differences between joint angles and limb orientation angles ($\alpha=0.05$). We performed a single factor ANOVA for each total variance measurement (limb orientation and pooled joint angles) over the data collection stages (pre-injury, paralytic stage, and self-reinnervated stage) to test for an effect over time. When we detected a significant effect, we performed a Tukey–Kramer HSD *post-hoc* test to further discriminate between time stages.

To gain additional insight into the relative influence of individual limb elements on whole limb position, we created two mathematical functions that related the five limb segment angles of our hindlimb

kinematics model (Θ_S, measured in the same global reference system as limb orientation) to either limb orientation (θ_L, Eqn 1) or limb length ($\mathbf{L}_L$, Eqn 2):

$$\theta_L = \mathbf{J}(\theta) \times \theta_S \quad (1)$$

$$\mathbf{L}_L = \mathbf{J}(\theta) \times \theta_S\,, \quad (2)$$

where $\mathbf{J}$ is a 1×5 Jacobian matrix of partial derivatives relating small changes in each segment angle relative to the horizontal (forefoot, hindfoot, shank, thigh and pelvis) to small changes in the limb level variable, limb orientation (θ_L) or limb length ($\mathbf{L}_L$). Since the orientation of each limb segment with the horizontal determines the orientation and length of the entire limb, we performed an analysis examining the values of each cell of the two Jacobian matrices relating the segment of each limb to overall limb orientation (length). These values provided an indication of how much the variation of each segment angle will affect the limb orientation (length). Because these effects depend on the geometry of the limb, the average values were computed for each percentage of the time normalized gait cycle. Quantifying the relative influence of each segment angle on the limb kinematics gave us general insights to complement our joint angle variance data. Using averaged kinematics data for each cat and condition, we calculated the coefficients of the Jacobian ($\mathbf{J}$) over the entire step cycle. This provided a quantitative comparison of the relative influence of each segment angle on either limb orientation or limb length and how these sensitivities changed after injury.

RESULTS

Mean joint angle trajectories

Prior to peripheral nerve injury, our joint kinematics data were comparable with data reported in the literature for healthy intact cat locomotion (Goslow et al., 1973; Maas et al., 2007; Smith et al., 1998). Post-injury, we observed clear changes in mean joint kinematics trajectories for each cat compared with pre-injury (Fig. 3). Nerve injuries to ankle extensor muscles had clear effects on other joints of the limb. The directions and magnitudes of joint deficits after injury, however, could sometimes be unpredictable depending on injury condition and animal.

As expected, paralyzed triceps surae muscles resulted in a large ankle flexion, or yield, during the weight acceptance period of the stance phase (Fig. 3). This was consistent across all three triceps-injured animals. In these animals, the other joints of the limb were also affected in response to the altered ankle kinematics. Notably, the MTP and hip joint trajectories of all three triceps-injured cats showed the same changes with greater MTP flexion and hip extension throughout the stance phase compared with pre-injury. By contrast, the knee joint trajectory showed some variation with cat 4 showing relatively little effect at the knee whereas cats 3 and 5 showed increased peak knee extension during the paralytic stage. With muscle self-reinnervation, there were fewer consistent trends across individuals. For example, MTP joint trajectories of the three triceps-injured cats showed three different patterns after muscle self-reinnervation (Fig. 3).

The soleus nerve injury group displayed more subtle deficits at both paralytic and self-reinnervated stages. We still observed notable deficits at the MTP joint, but they were not consistent between animals. MTP kinematics of the two soleus-injured animals provided an exemplary case of inter-animal variability after nerve injury (Fig. 3, two bottom-left panels). Cat 1 showed a clear post-injury response favoring decreased (more hyper-extended) MTP joint angles across the gait cycle. By contrast, Cat 2 adopted increased (less hyper-extended) MTP joint angles. Differences in MTP kinematics remained after soleus self-reinnervation.

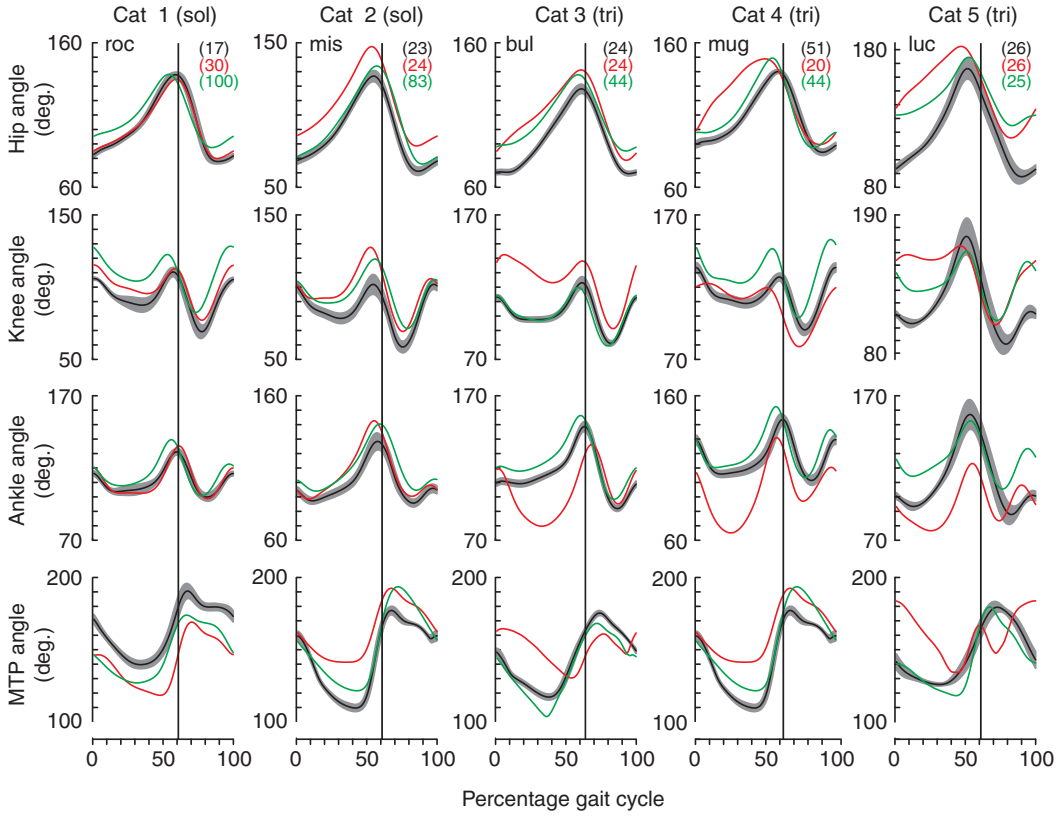

Fig. 3. Mean joint angle trajectories over 14 months of study show a wide variety of deficits at each joint for each cat and post-injury stage. Mean control data (black solid lines) ±1 s.d. (gray shading) are compared with mean data from the paralytic stage (red lines) and self-reinnervated stage (green lines). Larger included joint angles represent greater joint extension in all joints except the MTP joint, which is naturally in a state of hyperextension in the cat. For the MTP joint smaller angles indicate more hyperextension. Number of step cycles for each mean trajectory is shown in parentheses. Vertical lines indicate transition from stance phase to swing phase of gait.

Interjoint coordination was affected by both muscle paralysis and self-reinnervation. We observed drastic changes as indicated by angle–angle plots during the paralytic stage, followed by more subtle post-injury changes in joint range of motion during the self-reinnervated stage (Fig. 4). These data suggest relatively unique post-injury mean joint kinematics for each animal. In cat 3 for example, stance phase knee joint range of motion returned to normal after triceps surae self-reinnervation (shaded regions in Fig. 4A,B) while baseline shifts occurred in hip and ankle joint ranges of motion. By contrast, with the same injury cat 4 preserved stance phase hip and ankle joint ranges of motion while that of the knee shifted (shaded regions in Fig. 4D,E).

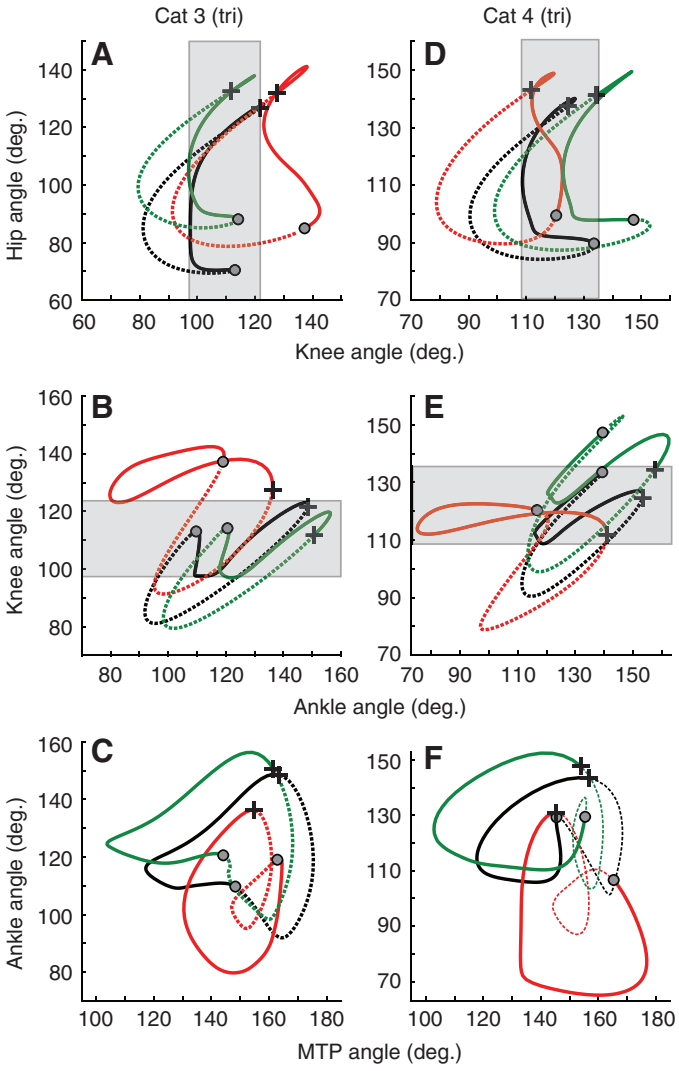

Fig. 4. Angle–angle plots from two representative cats with the same triceps surae nerve injury reveal distinctly different interjoint compensation patterns after injury. Mean control data (black) are plotted with data from the paralytic (red) and the self-reinnervated stages (green). Stance phases (solid lines) begin with paw contact (filled circles) and swing phases (dashed lines) begin with paw liftoff (crosses). After self-reinnervation, cat 3 (A–C) returned to pre-injury stance phase knee joint range of motion (gray shading) while obvious deficits in joint range of motion remained at the hip, ankle and MTP joints. Cat 4 (D–F) preserved ankle and hip joint ranges of motion while allowing range of motion deficits at the knee and MTP joints. Data are from the same step cycles shown in Fig. 3.

Mean limb orientation and limb length trajectories

Mean kinematics trajectories of limb orientation and limb length were far less affected after nerve injury compared with individual joints (Fig. 5). Mean limb orientation trajectories of all cats followed the same pattern and magnitudes of stance phase retraction and swing phase protraction across all injury conditions. Mean limb length trajectories before and after injury displayed a brief period of limb shortening during the initial weight-bearing, or yield, phase of stance followed by lengthening throughout the rest of stance. Mean limb length dramatically shortened over the first half of swing phase and extended as it approached paw contact of the next stride cycle. Despite small post-injury differences, these trajectory patterns were well conserved across all animals in both shape and magnitude.

Consistency of mean kinematics trajectories after injury

Post-injury kinematics data matched pre-injury data better for limb orientation and limb length trajectories than for individual joint angles. A linear regression of post-injury mean kinematics trajectories as a function of mean pre-injury kinematics provided a quantitative metric of the consistency of the trajectory pattern after nerve injury (Fig. 6). A perfectly unchanged mean trajectory would correspond to a regression that matches the line of identity, or an R^2=1.0. A post-injury mean trajectory that did not match pre-injury kinematics would result in a R^2 equal to zero. R^2 values averaged across all animals ($\bar{R}^2$) indicated invariant mean limb kinematics after injury (Fig. 7). During the paralytic stage, only limb orientation ($\bar{R}^2$=0.93±0.89, P=0.0002) and limb length ($\bar{R}^2$=0.82±0.11, P=0.0017) kinematics were preserved ($\bar{R}^2$>0.50) over the yield phase of stance and only limb orientation ($\bar{R}^2$=0.99±0.002, P<0.0001) was preserved over the entire stance phase. After muscle self-reinnervation, $\bar{R}^2$ values of both limb orientation (0.91±0.09, P=0.0012) and limb length (0.84±0.14, P=0.0094) remained high over the yield phase. After self-reinnervation, both limb orientation ($\bar{R}^2$=0.97±0.05, P=0.0001) and limb length ($\bar{R}^2$=0.83±0.24, P=0.0352) trajectories were preserved over the entire stance phase.

In comparison, no individual joint angle trajectories were preserved during the paralytic stage (Fig. 7). After self-reinnervation, only the knee joint trajectory over the yield phase had returned for all cats ($\bar{R}^2$=0.77±0.20, P=0.0373) but a normal knee joint trajectory did not persist over the entire stance phase ($\bar{R}^2$=0.54±0.32, P=0.4014). R^2 values for ankle joint ($\bar{R}^2$=0.69±0.46, P=0.2375) and hip joint ($\bar{R}^2$=0.24±0.48, P=0.8208) trajectories, in contrast, were not high for all cats over the yield phase of stance, but were over the remainder of stance phase ($\bar{R}^2$=0.81±0.24, P=0.0389; and $\bar{R}^2$=0.95±0.06, P=0.0004, respectively).

Variance of joint and limb kinematics across step cycles

Regardless of the type of injury, the individual joints of the hindlimb exhibited greater step-by-step variability than the entire limb. At each of the pre-injury, paralytic and self-reinnervated stages, the cumulatively summed variance, or total variance, of individual joint angles was always greater than the total variance of limb orientation (Fig. 8). Prior to nerve injury, intact cats exhibited greater total variance in individual joint angles (0.58±0.57 rad^2) compared with the total variance of limb orientation (0.25±0.14 rad^2, P=0.027). All animals during the paralytic stage also exhibited greater joint angle total variance (0.80±0.24 rad^2) compared with limb orientation total variance (0.37±0.24 rad^2, P=0.016). After muscle self-reinnervation, all animals again demonstrated greater total variance in joint kinematics (1.49±0.87 rad^2) compared with total variance of limb orientation (0.53±0.27 rad^2, P<0.001).

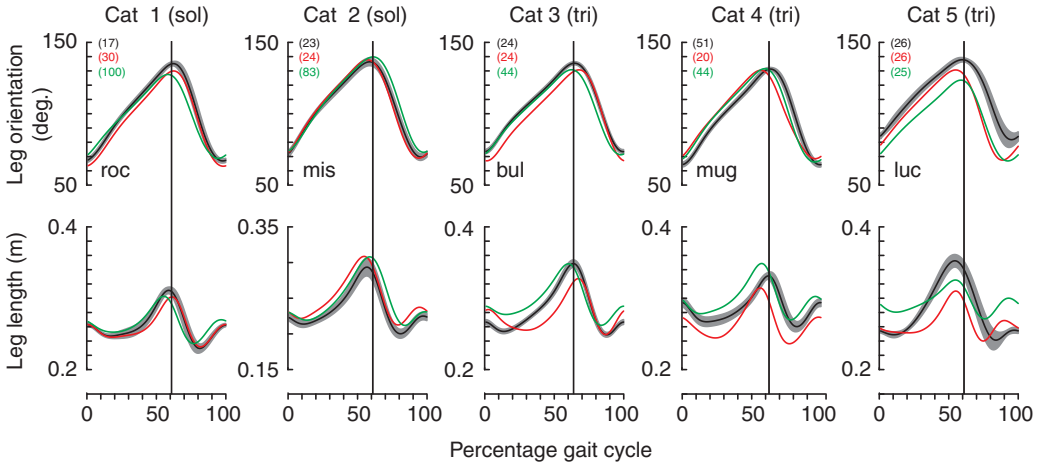

Fig. 5. Across all five cats, mean limb length and limb orientation trajectories over 14 months of study showed a notable trend for conservation of the pre-injury trajectory. Data are from the same step cycles shown in Fig. 3 and follow the same legend.

The total variance of limb orientation did not change after injury as a result of muscle paralysis or self-reinervation [$F_{(3,15)}$=1.95, P=0.18]. The step-by-step total variance of joint angles, however, did increase after injury [$F_{(3,60)}$=10.07, P<0.001]. Although total variance of joint angles increased in both post-injury stages, only the self-reinnervated stage was significantly different (α=0.05; Fig. 8).

Step-by-step deviations observed at the limb level were not equally sensitive to the deviations of individual limb elements. Limb orientation was most sensitive to deviations in shank and thigh segment angles, and least sensitive to deviations of the forefoot and pelvis angles (Fig. 9A). Positive values of limb orientation sensitivity indicated that an increase in any of the five segment angles would result likewise in an increase in limb orientation. Although the relative magnitudes of sensitivity were modulated across the gait cycle, individual patterns changed little after injury (Fig. 9A–C) and were similar across all cats (Fig. 9D,E). Limb length was also most sensitive to shank and thigh angle deviations, however, these had opposite effects as indicated by the opposite signs for sensitivity (Fig. 9F). This means an increase in shank segment angle would increase limb length, whereas the same increase in thigh segment angle would decrease limb length.

DISCUSSION

Changes in mean joint kinematics trajectories after peripheral nerve injury

In a given animal, peripheral nerve injury results in clear changes to mean joint kinematics, which are often referred to as locomotor deficits in cases of pathological gait. Although varied responses occur between animals at some joints, some consistent trends also exist. The magnitude of the joint deficit is related to the severity of the injury. Paralysis resulted in greater changes to mean joint angles compared with self-reinnervation. The polyarticular characteristics of remaining unaffected muscles also had an effect on resulting joint deficits.

A large biomechanical constraint exists when the plantaris muscle remains as the only major ankle extensor as a result of paralyzed triceps surae muscles. Although extrinsic foot muscles such as flexor hallucis longus can be significant contributors to ankle extension (Lawrence et al., 1993), the larger plantaris muscle with its substantial ankle extensor muscle moment arm probably takes over the majority of ankle extension duties when the triceps surae group is paralyzed. The plantaris muscle is a powerful ankle extensor used during normal cat locomotion (Prilutsky et al., 1996), however, it is also a significant flexor of the MTP joint because of its continuous insertion onto the flexor digitorum brevis muscle (Crouch, 1969). Owing to this triarticular nature, an increased ankle extensor role for plantaris would create a biomechanical coupling between the ankle and MTP joints such that greater ankle extension would correlate with greater MTP angles (i.e. less hyperextension). As expected, all three triceps surae-paralyzed animals displayed increases in MTP joint angles because of the increased role played by the plantaris muscle as an ankle extensor. When only soleus is paralyzed, it is possible for either the triarticular plantaris or biarticular gastrocnemius muscles to take over any lost ankle extensor function. Cat 2 showed the same increase in MTP joint angles as the triceps injured cats suggesting this animal probably relied more on plantaris after injury. By contrast, cat 1 displayed smaller MTP joint angles (i.e. increased hyperextension) suggesting more reliance on the gastrocnemius muscle at the ankle joint, which does not cross the MTP joint.

With muscle self-reinnervation, mean joint angle trajectories approach more normal, pre-injury kinematics compared with the paralytic stage, but some deficits remain (Fig. 7). After great disruption during the paralytic stage, interjoint coordination approaches pre-injury values after self-reinnervation with some lingering deficits in mean joint kinematics (Fig. 4). These lingering joint deficits become more obvious and consistent across animals when these cats walk down an incline (Abelew et al., 2000; Maas et al., 2007) because of the greater reliance on length and force feedback, which are effectively lost after muscle self-reinnervation (Cope et al., 1994). Although mean joint kinematics are altered during level walking, individual cats exhibit individual variation in mean kinematics patterns over the gait cycle.

Invariance of mean limb kinematics after peripheral nerve injury

In contrast to the joint kinematics, mean trajectories of the limb kinematics are highly conserved across animals after peripheral nerve injury. Pre-injury mean limb orientation and limb length trajectories persist during both paralytic and self-reinnervated stages (Figs 5 and 6). Maintaining the same limb position trajectory is of primary importance during locomotion after neuromuscular injury. Furthermore, these data suggest that preservation of pre-injury limb orientation and limb length trajectories is accomplished through the long-term compensatory changes occurring across all of the individual joints. This long-term compensation strategy exploits the neuromechanical redundancy in the limbs to coordinate different combinations of joint angles that result in the same net global limb kinematics (Fig. 8). We see this to be the case in four different

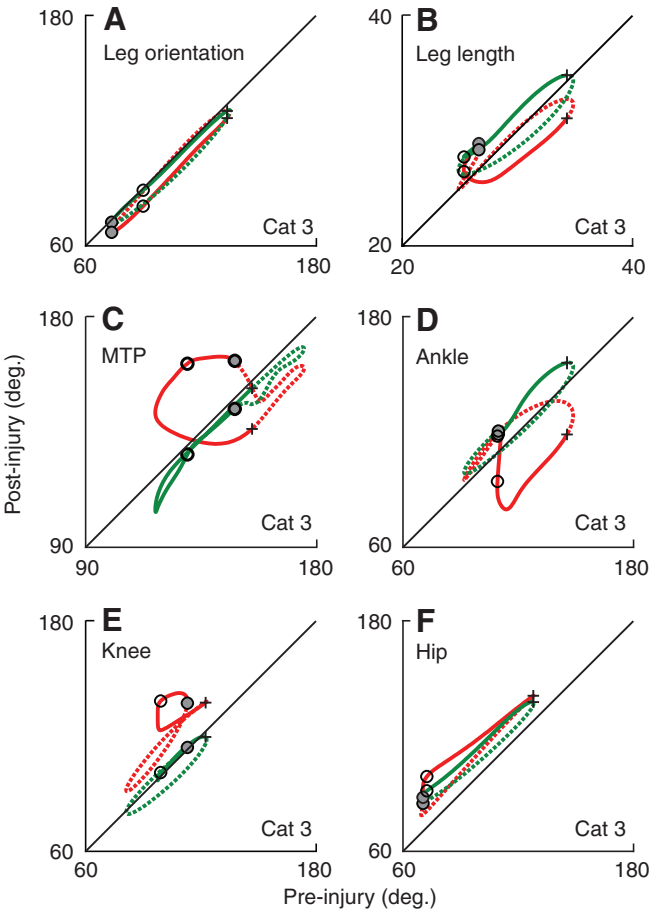

Fig. 6. General limb position kinematics (A,B) and individual joint kinematics (C–F) from a representative cat with a triceps surae muscle nerve injury. Paralytic stage (red) and self-reinnervated stage (green) mean trajectory data are plotted as a function of its corresponding pre-injury data. Deviations from lines of identity (black line) indicate differences from the pre-injury control strategy. Stance phases (solid lines) and swing phases (dashed lines) are indicated with designated times of paw contact (filled circles), terminations of the yield phase (open circles) and beginnings of swing phase (crosses). Data are means of 24 and 44 cycles for the paralytic and self-reinnervated stages, respectively.

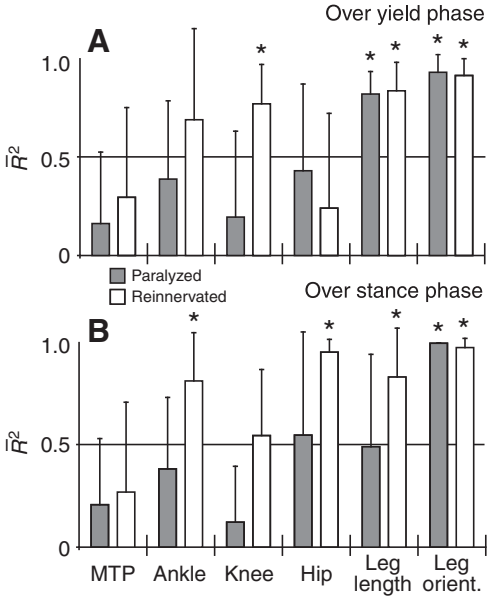

Fig. 7. Average coefficient of determination across all cats ($\bar{R}^2$) for different kinematics variables at the paralytic stage (shaded bars) and the self-reinnervated stage (open bars). R^2 for each cat was calculated from trajectory comparisons (regressions) made over the weight acceptance portion of stance (A) and over the entire stance phase (B). Data are mean values ± s.d. across all animals. *R^2>0.50 for linear regression of post-injury kinematics trajectory as a function of pre-injury kinematics (P<0.05).

neuromuscular injury conditions: soleus muscle paralysis, soleus muscle self-reinnervation, triceps surae group paralysis, and triceps surae group self-reinnervation. This suggests that the coordination of joint kinematics to preserve limb kinematics may be a fundamental guiding principle of long-term locomotor compensation in cats.

At the joint-level, there is no return to pre-injury mean joint angle trajectories during the paralytic stage. After self-reinnervation, only three instances of joint angle trajectory are preserved. After self-reinnervation, mean knee angle trajectory returns to its pre-injury state, but only over the yield phase (Fig. 7A). When we consider the rest of stance phase, only mean ankle and hip joint kinematics return to pre-injury states (Fig. 7B). These data suggest the knee joint may have an important function during the yield phase of stance and that the ankle and hip joints may be critical over the remainder of stance. These notions, however, require further testing to confirm. The lack of persistence of any joint angle trajectories during the paralytic stage, however, suggests that maintaining joint-level tasks are of secondary importance relative to maintaining invariant limb function.

Similarities in long-term and short-term locomotor compensation strategies

Our long-term compensation data suggest that after neuromuscular injury, different individual cats will arrive at different solutions, or combinations of joint kinematics patterns, that satisfy the common goal of maintaining invariant limb kinematics. These joint-level kinematic changes occur over weeks and months while accommodating the changing sensorimotor abilities associated with peripheral nerve injury and recovery. Long-term locomotor compensation to chronically adjust mean joint kinematics in this way could utilize a pre-existing short-term compensation strategy that explores and exploits numerous possible combinations of joint angles to minimize variability of limb kinematics on a step-by-step basis.

In addition to a long-term compensation strategy that uses altered mean joint angle trajectories to maintain invariant mean limb kinematics, we found a short-term compensation strategy that minimizes step-by-step variability of limb kinematics despite an increase in joint angle variability. Step-by-step total variance of all joint angles is consistently greater than total variance of limb orientation at all three injury stages. Limb orientation is sensitive to changes in each limb segment, so many combinations of joint deviations could result in increased limb total variance. Yet, this does not occur. Limb orientation is defined kinematically by the net combination of joint angles and segment lengths. Although joint angles vary significantly from one step to the next, they are selected in combinations that tend to keep overall limb orientation invariant. A short-term compensation strategy to decrease step-by-step limb variability is similar in concept to the long-term compensation strategy that preserves mean limb kinematics trajectories through the selection of appropriate mean joint kinematics. In both cases, redundancy in joint angle combinations that result in the same net

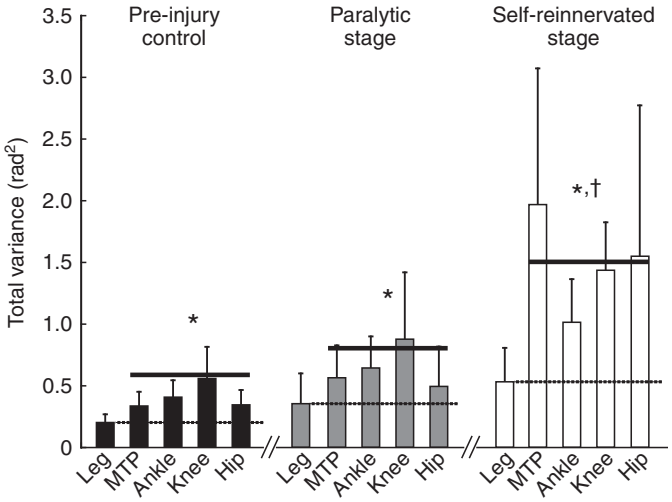

Fig. 8. Ensemble means across all cats of the total variance of different variables measured pre-injury (black bars), at the paralytic stage (shaded bars) and at the self-reinnervated stage (open bars). At each stage, total variance of individual joint angles was always greater than the variance of the limb orientation (horizontal dotted lines) regardless of injury status. Bars represent means ± s.d. across all animals for the variance cumulatively summed over each gait cycle for all strides. *Significant difference between total variance of all joints (horizontal solid lines) and total variance for limb orientation at each injury stage (P<0.05). †Significant difference from pre-injury control (P<0.05).

limb position is exploited to overcome challenges due to nerve injuries occurring over months or natural step-by-step variations occurring over seconds.

Surprisingly, the step-by-step joint variance increased throughout the study period, or across injury stages (Fig. 8). One might have predicted that step-to-step variance might come back to pre-injury levels with muscle self-reinnervation, especially since the mean joint trajectories returned closer to pre-injury values. One possible explanation for this is that the cats had increased their reliance on using joint covariance after injury to maintain a consistent limb kinematics trajectory. Although there is some evidence of increased goal-equivalent joint variability with pathological gait (Black et al., 2007), this is a relatively unexplored area and deserves further attention. The finding that consistent limb kinematics are achieved through greater joint variability provides interesting evidence that the recovery process after injury does not include returning to the same neuromuscular state before injury. Locomotor recovery may then be more appropriately viewed as the persistence of limb-level function through enhancement of joint-level compensatory processes, or altered motor control strategies. The ability for locomotor compensation could be a heritable form of behavioral plasticity and represent an evolutionary adaptation for physiologically adaptive behavior (Bronmark and Miner, 1992; Bronmark and Pettersson, 1994; Gotthard and Nylin, 1995; Wagner, 1996). Although an intriguing possibility, to thoroughly test such an idea would require much more work than is possible here.

Limb kinematics may be guiding the selection of joint angle combinations

Deliberation over what guides these compensatory responses after injury may require a broader view of what functional tasks are being met with each step. Although a peripheral nerve injury may directly affect only muscles acting at the ankle joint, concomitant responses occur across all major joints of the limb. An appealing proposition is that stabilization of limb-level kinematics alone are attended to at higher supraspinal levels of the nervous system. These limb-level control signals then descend and guide lower levels of organization that select and regulate individual joint kinematics through a more automated process. The anatomical locations of these higher-level control centers are unknown, but remain an active area of research (Drew et al., 2008; Ting, 2007; Ting and McKay, 2007). At lower levels of the locomotor system, regulation of joint kinematics to consistently satisfy higher-level commands might include a mixture of active neural processes, such as autogenic and heterogenic spinal reflex pathways, and passive biomechanical mechanisms, such as the mechanical coupling associated with biarticular muscles and interaction torques. It is likely that both active and passive mechanisms are involved.

Preferential conservation of limb-level kinematics over joint-level kinematics over long and short time scales suggests that a neuromechanical representation of whole limb function may guide joint-level locomotor compensations. This intralimb compensation mechanism exploits the abundance of joint-angle combinations that are goal-equivalent for the limb-level tasks of orientation and length control. With muscle paralysis, when none of the individual joints could match pre-injury kinematics, limb-level function remained invariant across all cats (Fig. 7). Although the functional role of individual joint trajectories over the stance phase may require more study, the persistence of joint-level function appeared to be of secondary importance compared with the preservation of whole limb function.

Our findings support previous work that suggests neural representations of whole limb position (orientation and length) in the cat are encoded at the level of the spinal cord (Bosco and Poppele, 2000; Bosco and Poppele, 2003; Bosco et al., 2000). This sensory representation of whole limb position ascends spinal tracts to higher brain centers and is probably an important determinant of locomotor control of the limbs. Recent work also suggests that the increased cortical activity associated with more complex walking tasks is due to modifications made during gait (Beloozerova and Sirota, 1993a; Beloozerova and Sirota, 1993b; Beloozerova and Sirota, 1998; Drew et al., 2008). This suggests the central nervous system may use neural representations of limb-level kinematics to assemble goal-equivalent, joint-level compensatory responses that correct and stabilize normal limb function on a step-by-step basis, both before and after injury.

Both neural and mechanical processes may regulate these immediate joint-level compensations. Heterogenic force feedback pathways can contribute to such a compensation mechanism between muscles crossing adjacent joints. Heterogenic reflex pathways that affect the knee and ankle joints have been identified in the cat to affect interjoint coordination (Nichols et al., 1999; Wilmink and Nichols, 2003). For example, increased force production in the triceps surae muscles related to inadvertent ankle extension would increase inhibition of the quadriceps muscles and result in a compensatory decrease in knee extension. A recent modeling study of the cat hindlimb indicates heterogenic reflexes result in greater stability or maintenance of limb position against perturbations (Bunderson et al., 2007). These and other yet to be identified reflex pathways probably function to regulate automatic joint-level responses to preserve goal-equivalence at the limb level.

In addition to neural mechanisms, passive mechanics may improve compensatory action in the joints. The role of biarticular muscles and interaction torques across limb segments is implicated

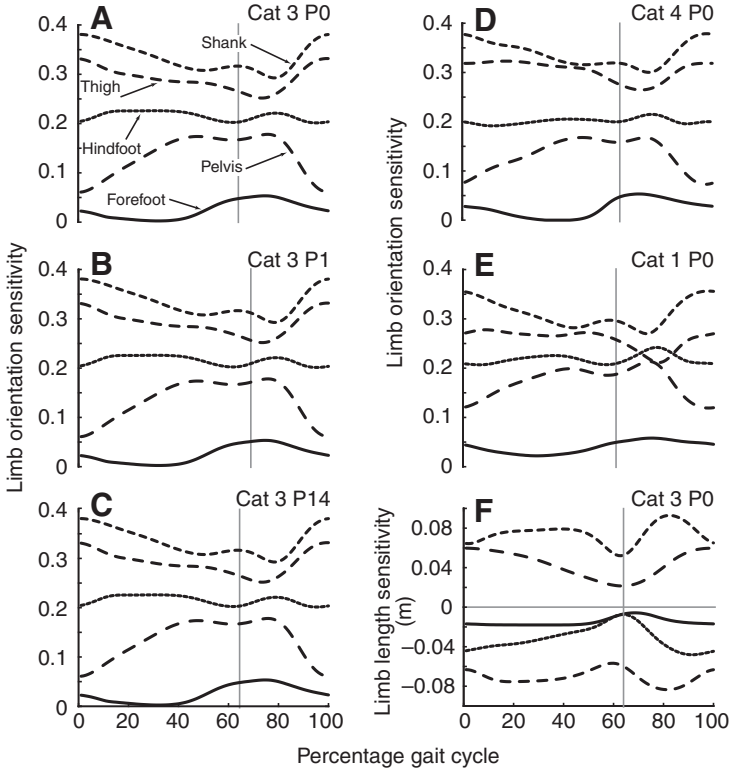

Fig. 9. Sensitivity of limb level variables to deviations in segment angles. Limb orientation sensitivities for pre-injury control (A), with paralyzed triceps surae (B), and self-reinnervated triceps surae muscles (C) from the same animal show little change in relative influence as a result of nerve injury. Pre-injury limb orientation sensitivities from two other animals (D,E) show that the influence of an individual segment angle is comparable across animals. (F) Limb length sensitivity from same animal as in A–C shows a different pattern of relative influences of segment angles on limb length. Positive sensitivity indicates that a small positive change in segment angle results in a positive change in limb orientation (A–E) or limb length (F). Solid line indicates the distal-most segment (forefoot) and lines of increasingly larger dashes representing more proximal segments of our kinematics model. Vertical gray line indicates beginning of swing phase.

in stabilizing the shoulder-elbow complex in arm reaching movements (Cabel et al., 2001; Kurtzer et al., 2006; Sangani et al., 2007) and in helping explore goal-equivalent kinematic solutions during other human arm movements (Martin et al., 2009). In human hopping, simply adopting a more extended limb position can help stabilize limb-level force production on the ground despite high joint torque variances (Yen and Chang, in press).

The invariance of whole limb function that results from joint-level compensatory actions may also help explain why simple biomechanical models, such as the inverted pendulum model for walking and the spring-mass model for running, can robustly predict the dynamics of legged locomotion across so many species with complex and different morphologies (Blickhan, 1989; Full and Koditschek, 1999; McMahon, 1990; Srinivasan and Ruina, 2006). These biomechanical models grossly oversimplify the complex neuromusculoskeletal features of the limbs during locomotion. Yet, along with the studies suggesting neural representations of whole limb position, our results suggest these simple biomechanical templates for limb function may reflect actual performance variables controlled by higher levels of the locomotor system.

A coordinated, joint-level response can minimize the effect of limb-destabilizing deviations experienced by any single joint. For example, humans minimize the variability of end-point position or end-point force by exploiting goal-equivalent variability in the joints during upper extremity reaching movements (Scholz and Schöner, 1999; Tseng et al., 2002; Tseng and Scholz, 2005) and finger force production tasks (Kang et al., 2004; Shinohara et al., 2003; Shinohara et al., 2004), respectively. In a locomotor task, similar compensation strategies exist for lower limb control during human hopping (Auyang et al., 2009; Yen et al., 2009) (Yen and Chang, in press). Humans hopping in place coordinate joint-level kinematics to minimize the effects of natural cycle-to-cycle joint-level variance on limb orientation and limb length (Auyang et al., 2009). To the best of our knowledge, this is the first evidence that task-oriented goals such as limb position in the cat may be driving joint-level locomotor compensations after neuromuscular injury.

In summary, limb-level kinematics are preferentially maintained over individual joint-level kinematics after multiple types of peripheral nerve injury in cat ankle extensor muscles. Limb orientation and limb length are functionally relevant locomotor tasks stabilized by goal-equivalent compensatory actions at the joints and appear to guide long-term locomotor compensation after injury and short-term locomotor compensation on a step-by-step basis. This suggests animals exploit motor redundancy in the limbs to stabilize limb function with each step, and that this compensation strategy can persist over temporary and permanent disruptions of joint function.

We would like to give special thanks to Thom Abelew, Andrea Burgess, Jinger Gottschall, Clotilde Huyghues-Despointes, Melissa Miller, Bin Nguyen, Kyla Ross, and David Spinner for their invaluable assistance in collecting, digitizing and analyzing the data for this study. We would also like to thank Teresa Snow for her statistics advice, Thomas Roberts for help with the knee triangulation technique and the members of the Comparative Neuromechanics Laboratory for their helpful comments on this manuscript. This work was supported in part by NIH AR054760-01 (to Y.H.C.), NIH NS043893-01A1 (to Y.H.C.), NIH HD32571-06A1 (to T.R.N.) and NSF 0078127 and NIH NS050880-05 (to J.P.S.). Deposited in PMC for release after 12 months.

REFERENCES

Abelew, T. A., Miller, M. D., Cope, T. C. and Nichols, T. R. (2000). Local loss of proprioception results in disruption of interjoint coordination during locomotion in the cat. *J. Neurophysiol.* **84**, 2709-2714.

Auyang, A. G., Yen, J. T. and Chang, Y. H. (2009). Neuromechanical stabilization of leg length and orientation through interjoint compensation during human hopping. *Exp. Brain. Res.* **192**, 253-264.

Beloozerova, I. N. and Sirota, M. G. (1993a). The role of the motor cortex in the control of accuracy of locomotor movements in the cat. *J. Physiol.* **461**, 1-25.

Beloozerova, I. N. and Sirota, M. G. (1993b). The role of the motor cortex in the control of vigour of locomotor movements in the cat. *J. Physiol.* **461**, 27-46.

Beloozerova, I. N. and Sirota, M. G. (1998). Cortically controlled gait adjustments in the cat. *Ann. NY Acad. Sci.* **860**, 550-553.

Black, D., Smith, B., Wu, J. and Ulrich, B. (2007). Uncontrolled manifold analysis of segmental angle variability during walking: preadolescents with and without Down syndrome. *Exp. Brain Res.* **183**, 511-521.

Blickhan, R. (1989). The spring-mass model for running and hopping. *J. Biomech.* **22**, 1217-1227.
Bosco, G. and Poppele, R. E. (2000). Reference frames for spinal proprioception: kinematics based or kinetics based? *J. Neurophysiol.* **83**, 2946-2955.
Bosco, G. and Poppele, R. E. (2003). Modulation of dorsal spinocerebellar responses to limb movement. II. Effect of sensory input. *J. Neurophysiol.* **90**, 3372-3383.
Bosco, G., Poppele, R. E. and Eian, J. (2000). Reference frames for spinal proprioception: limb endpoint based or joint-level based? *J. Neurophysiol.* **83**, 2931-2945.
Bronmark, C. and Miner, J. G. (1992). Predator-induced phenotypic change in body morphology in crucian carp. *Science* **258**, 1348-1350.
Bronmark, C. and Pettersson, L. B. (1994). Chemical cues from piscivores induce change in morphology in crucian carp. *Oikos* **70**, 396-402.
Bunderson, N. E., Ting, L. H. and Burkholder, T. J. (2007). Asymmetric interjoint feedback contributes to postural control of redundant multi-link systems. *J. Neural Eng.* **4**, 234-245.
Cabel, D. W., Cisek, P. and Scott, S. H. (2001). Neural activity in primary motor cortex related to mechanical loads applied to the shoulder and elbow during a postural task. *J. Neurophysiol.* **86**, 2102-2108.
Cavagna, G. A., Heglund, N. C. and Taylor, C. R. (1977). Mechanical work in terrestrial locomotion: two basic mechanisms in minimizing energy expenditure. *Am. J. Physiol.* **233**, R243-R261.
Cope, T. C. and Clark, B. D. (1993). Motor-unit recruitment in self-reinnervated muscle. *J. Neurophysiol.* **70**, 1787-1796.
Cope, T. C., Webb, C. B. and Botterman, B. R. (1991). Control of motor-unit tension by rate modulation during sustained contractions in reinnervated cat muscle. *J. Neurophysiol.* **65**, 648-656.
Cope, T. C., Bonasera, S. J. and Nichols, T. R. (1994). Reinnervated muscles fail to produce stretch reflexes. *J. Neurophysiol. (Bethesda)* **71**, 817-820.
Crouch, J. E. (1969). *Text-Atlas of Cat Anatomy.* Philadelphia: Lea & Febiger.
Drew, T., Kalaska, J. and Krouchev, N. (2008). Muscle synergies during locomotion in the cat: a model for motor cortex control. *J. Physiol.* **586**, 1239-1245.
English, A. W. (2005). Enhancing axon regeneration in peripheral nerves also increases functionally inappropriate reinnervation of targets. *J. Comp. Neurol.* **490**, 427-441.
Fowler, E. G., Gregor, R. J., Hodgson, J. A. and Roy, R. R. (1993). Relationship between ankle muscle and joint kinematics during the stance phase of locomotion in the cat. *J. Biomech.* **26**, 465-483.
Full, R. J. and Koditschek, D. E. (1999). Templates and anchors: neuromechanical hypotheses of legged locomotion on land. *J. Exp. Biol.* **202**, 3325-3332.
Goslow, G. E., Jr, Reinking, R. M. and Stuart, D. G. (1973). The cat step cycle: hind limb joint angles and muscle lengths during unrestrained locomotion. *J. Morphol.* **141**, 1-41.
Gotthard, K. and Nylin, S. (1995). Adaptive plasticity and plasticity as an adaptation: a selective review of plasticity in animal morphology and life history. *Oikos* **74**, 3-17.
Griffin, T. M., Main, R. P. and Farley, C. T. (2004). Biomechanics of quadrupedal walking: how do four-legged animals achieve inverted pendulum-like movements? *J. Exp. Biol.* **207**, 3545-3558.
Huyghues-Despointes, C., Cope, T. C. and Nichols, T. R. (2003a). Intrinsic properties and reflex compensation in reinnervated triceps surae muscles of the cat: Effect of activation level. *J. Neurophysiol.* **90**, 1537-1546.
Huyghues-Despointes, C., Cope, T. C. and Nichols, T. R. (2003b). Intrinsic properties and reflex compensation in reinnervated triceps surae muscles of the cat: Effect of movement history. *J. Neurophysiol.* **90**, 1547-1555.
Institute for Laboratory Animal Research (1996). *Guide for the Care and Use of Laboratory Animals*. Washington, DC: National Academy Press.
Kang, N., Shinohara, M., Zatsiorsky, V. M. and Latash, M. L. (2004). Learning multi-finger synergies: an uncontrolled manifold analysis. *Exp. Brain Res.* **157**, 336-350.
Kram, R., Griffin, T. M., Donelan, J. M. and Chang, Y. H. (1998). Force treadmill for measuring vertical and horizontal ground reaction forces. *J. Applied Physiol.* **85**, 764-769.
Kurtzer, I., Pruszynski, J. A., Herter, T. M. and Scott, S. H. (2006). Primate upper limb muscles exhibit activity patterns that differ from their anatomical action during a postural task. *J. Neurophysiol.* **95**, 493-504.
Lawrence, J. H., III, Nichols, T. R. and English, A. W. (1993). Cat hindlimb muscles exert substantial torques outside the sagittal plane. *J. Neurophysiol.* **69**, 282-285.
Maas, H., Prilutsky, B. I., Nichols, T. R. and Gregor, R. G. (2007). The effects of self-reinnervation of cat medial and lateral gastrocnemius muscles on hindlimb kinematics in slope walking. *Exp. Brain Res.* **181**, 377-393.
Martin, V., Scholz, J.P. and Schoner, G. (2009). Redundancy, self-motion, and motor control. *Neural Comp.* **21**, 1371-1414.
McMahon, T. A. (1990). Spring-like properties of muscles and reflexes in running. In *Multiple Muscle Systems: Biomechanics and Movement Organization* (ed. J. M. Winters and S. L. Woo), pp. 578-590. New York: Springer-Verlag.
McMahon, T. A. and Cheng, G. C. (1990). The mechanics of running: how does stiffness couple with speed? *J. Biomech.* **23 (suppl. 1)**, 65-78.
Nichols, T. R. (1989). The organization of heterogenic reflexes among muscles crossing the ankle joint in the decerebrate cat. *J. Physiol.* **410**, 463-477.
Nichols, T. R. (1999). Receptor mechanisms underlying heterogenic reflexes among the triceps surae muscles of the cat. *J. Neurophysiol.* **81**, 467-478.
Nichols, T. R., Cope, T. C. and Abelew, T. A. (1999). Rapid spinal mechanisms of motor coordination. *Exerc. Sport Sci. Rev.* **27**, 255-284.
Prilutsky, B. I., Herzog, W. and Allinger, T. L. (1996). Mechanical power and work of cat soleus, gastrocnemius and plantaris muscles during locomotion: possible functional significance of muscle design and force patterns. *J. Exp. Biol.* **199**, 801-814.
Riley, P. O., Paolini, G., Della Croce, U., Paylo, K. W. and Kerrigan, D. C. (2007). A kinematic and kinetic comparison of overground and treadmill walking in healthy subjects. *Gait Posture* **26**, 17-24.
Sangani, S. G., Starsky, A. J., McGuire, J. R. and Schmit, B. D. (2007). Multijoint reflexes of the stroke arm: neural coupling of the elbow and shoulder. *Muscle Nerve* **36**, 694-703.
Scholz, J. P. and Schöner, G. (1999). The uncontrolled manifold concept: identifying control variables for a functional task. *Exp. Brain Res.* **126**, 289-306.
Shinohara, M., Li, S., Kang, N., Zatsiorsky, V. M. and Latash, M. L. (2003). Effects of age and gender on finger coordination in MVC and submaximal force-matching tasks. *J. Appl. Physiol.* **94**, 259-270.
Shinohara, M., Scholz, J. P., Zatsiorsky, V. M. and Latash, M. L. (2004). Finger interaction during accurate multi-finger force production tasks in young and elderly persons. *Exp. Brain. Res.* **156**, 282-292.
Smith, J. L., Carlson-Kuhta, P. and Trank, T. V. (1998). Forms of quadrupedal locomotion. III. A comparison of posture, hindlimb kinematics, and motor patterns for downslope and level walking. *J. Neurophysiol.* **79**, 1702-1716.
Srinivasan, M. and Ruina, A. (2006). Computer optimation of a minimal biped model discovers walking and running. *Nature* **439**, 72-75.
Ting, L. (2007). Dimensional reduction in sensorimotor systems: a framework for understanding muscle coordination of posture. *Prog. Brain Res.* **165**, 299-321.
Ting, L. and McKay, J. L. (2007). Neuromechanics of muscle synergies for posture and movement. *Curr. Opin. Neurobiol.* **17**, 622-628.
Tseng, Y. W. and Scholz, J. P. (2005). The effect of workspace on the use of motor abundance. *Motor Control* **9**, 75-100.
Tseng, Y., Scholz, J. P. and Schöner, G. (2002). Goal-equivalent joint coordination in pointing: affect of vision and arm dominance. *Motor Control* **6**, 183-207.
van Ingen, Schenau, G. J. (1980). Some fundamental aspects of the biomechanics of overground versus treadmill locomotion. *Med. Sci. Sports. Exerc.* **12**, 257-261.
Wagner, A. (1996). Does evolutionary plasticity evolve? *Evolution* **50**, 1008-1023.
Wilmink, R. J. and Nichols, T. R. (2003). Distribution of heterogenic reflexes among the quadriceps and triceps surae muscles of the cat hind limb. *J. Neurophysiol.* **90**, 2310-2324.
Yen, J. T., Auyang, A. G. and Chang, Y. H. (2009). Joint-level kinetic redundancy is exploited to control limb-level forces during human hopping. *Exp. Brain Res.* **196**, 439-451.
Yen, J. T. and Chang, Y.-H. (in press). Rate-dependent control strategies stabilize limb forces during human locomotion. *J. R. Soc. Interface.*